

Kinematics and origin of the ringed bipolar nebula Mz 1

A.P. Marston¹, M. Bryce², J.A. López³, J.W. Palmer², and J. Meaburn²

¹ Physics & Astronomy Department, Drake University, Des Moines, IA 50311, USA

² Physics & Astronomy Department, University of Manchester, Manchester M13 9PL, UK

³ Instituto de Astronomía, UNAM, Apdo. Postal 877, Ensenada, B.C. 22800, México

Received 23 July 1997 / Accepted 12 August 1997

Abstract. High resolution, spatially resolved measurements of the H α , [NII] 6584 Å and [SII] emission lines of the bipolar planetary nebula Mz 1 have been obtained with the Manchester Echelle Spectrometer on the Anglo-Australian telescope. The echelle profiles for slit positions that cross the central nebular core have been analysed and related to a previously obtained CCD image of the region. A well defined ‘ring like’ structure, readily apparent in our H α + [NII] image, is shown to be expanding with the main bulk of the nebula at 23 km s⁻¹ and in a manner which is well represented by a cylindrical model with expansion velocities proportional to the radial distance from centre to cylinder edge. The dynamical lifetime of the nebula is of the order of 7,000 years. Estimates of the electron density from [SII] emission-line ratios suggest a density in the ring of order 1700 cm⁻³ compared to 400 cm⁻³ in the rest of the nebular core. Combining this result with IRAS measurements, we estimate a mass of the nebula of order 0.5 M $_{\odot}$. We discuss the probable origin and history of the nebula in terms of interacting stellar winds and consider the bipolar nebula as having been formed either via a fast wind in an aspherical density distribution, or through a superwind confined by an equatorial disc. In either case a relatively high mass-loss rate ($\geq 5 \times 10^{-5}$ M $_{\odot}$ yr⁻¹) is inferred for the superwind phase prior to the existence of a fast wind phase of the current central star.

Key words: planetary nebulae: Mz 1 – stars: mass loss – ISM: jets and outflows

1. Introduction

Mz 1 ($\alpha_{(2000)}15:34:16.6$, $\delta_{(2000)}-59:08:59$) is a planetary nebula (PN) which has an ellipsoidal/bipolar shape with a ring of enhanced emission around its waist. Despite occurring in a number of catalogues (PN G 322.4-02.6, ARO 531, ESO 135-11, He 2-130, My 89, RCW 93, Sa 2-123, Wray 16-183) it seems to have been little studied. Distances to the PN are given by Van

de Steene & Zijlstra (1994) as 2.53 kpc, Cahn et al. (1992) as 2.28 kpc and Yhang (1995) as 2.85 kpc. These are all statistical distances and are based on the same data. The formalism of Van de Steene & Zijlstra (1994) assumes a diameter to the nebula of 25". From Fig. 1 this corresponds more closely to the radius rather than the diameter of Mz 1. Using the same formalism as Van de Steene & Zijlstra (1994) yields an improved distance of 2.0 kpc, which is the distance that will be adopted for the nebula throughout this paper. An uncertainty in this distance estimate is of order 30%.

In the majority of bipolar PNe, the kinematics of the expanding shell are characterised by outflows directed principally along the polar axes, and possibly ‘refracted’ flows along the walls of the expanding cavities. The origin of these morphological and kinematical properties is usually attributed to the “interacting winds” model Kwok et al. 1978. The formation of bipolar planetary nebulae via this model was predicted by Icke (1988), and this has been refined and confirmed by later numerical modeling (eg. Mellema 1993). Bipolarity is produced by the interaction of a fast wind with an equatorial density enhancement that leads to preferential expansion in the polar regions. In the case of Mz 1, the presence of a dense ring around the nebular equator could be interpreted as the remnants of this density enhancement. However, inconsistencies appear to exist with the above model and the new kinematical observations suggest other explanations for the origin of Mz 1.

2. Observations and results

An image of Mz 1 in the light of the H α and [NII] emission lines, obtained at the Las Campanas Observatory is presented in Fig. 1. The main body of the nebula can be described as a loose bipolar configuration marked by a conspicuous equatorial ring, which in projection appears to be elongated along PA 60° and whose major axis is approximately 30 arcsec long. This ring has a measured spatial aspect ratio of 3:2.

Spatially resolved [SII] and H α + [NII] profiles from Mz 1 were obtained with the Manchester Echelle Spectrometer Meaburn et al. 1984 in its primary mode at the f/8 focus of the Anglo-Australian Telescope (AAT) on the nights of 17 and 18

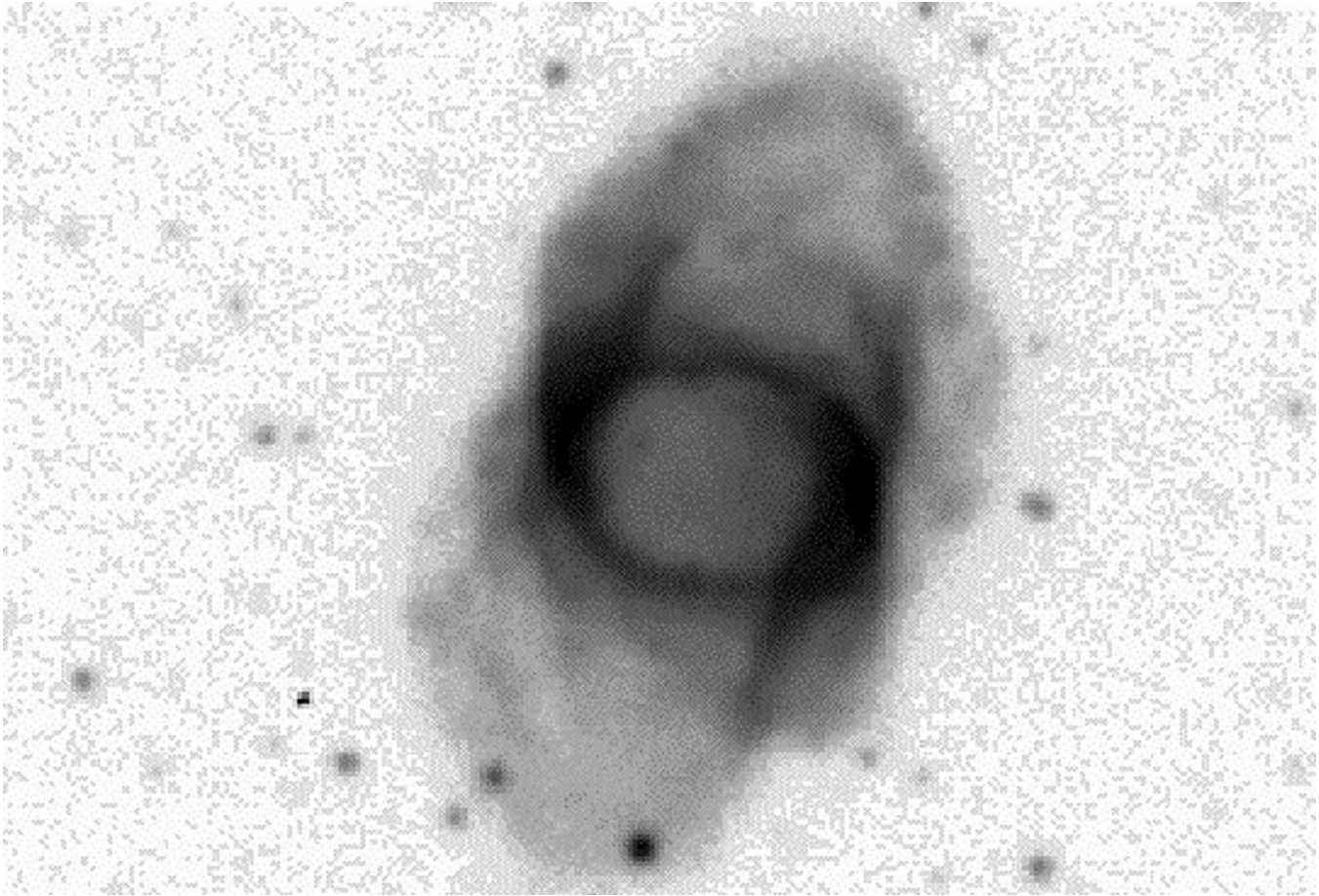


Fig. 1. $H\alpha$ + [NII] image of Mz 1. The image is 131 x 88 arcseconds.

Table 1. Observational details

Slit position	P.A.	Filter	integration (seconds)	seeing arcseconds
A	65°	$H\alpha$ + [NII]	600	3+
B	65°	$H\alpha$ + [NII]	1200	2
C	155°	$H\alpha$ + [NII]	1800	2
C	155°	[SII]	1100	2
D	155°	$H\alpha$ + [NII]	1800	2

February 1995. A single 150 μm slit was used giving a spectral HPBW of 9 km s^{-1} together with 100 \AA bandwidth filters centred on $H\alpha$, [NII] 6584 \AA and [SII] emission line wavelengths. The detector used in both sets of observations was the AAT TEK1 1024 \times 1024 Tektronix CCD. This was binned 2 \times 1 to give 512 spatial increments and 1024 bins in the dispersion direction. This set-up gives a spatial scale of 0.3185'' per increment (\equiv 0.031 pc) and a dispersion of \sim 0.05 \AA per channel around the observed wavelengths.

The slit positions are shown in Fig. 2. Details of slit orientation, filter, seeing and integration time are given in Table 1.

The data were analysed at the Manchester University STARLINK node using reduction programs from the FIGARO Shortridge 1991 and TWODSPEC Wilkins & Axon 1991 packages. The CCD frames were processed in the usual way and standard ThAr calibration spectra were used to re-bin the data to a linear wavelength scale.

The central region of Mz 1 presents a large dynamic range in surface brightness. Gaussian functions have been fitted to the extracted line profiles from every 8 consecutive increments co-added along the slit, in order to trace the separate velocity components within the main body of the nebula.

Some of the results from the longslit observations are displayed in Figs. 3 and 4. In Fig. 3 the [NII] 6584 \AA emission for each slit position are displayed as greyscale representations of emission intensity. A similar set of position/velocity arrays in the light of $H\alpha$, [NII] 6584 \AA and [SII] emissions for slit position C is presented in Fig. 4. The right hand panel represents the [SII] 6717 \AA over [SII] 6731 \AA position/velocity array. This result gives a pictorial indication of the relative electron densities present within the nebula. The darker areas indicate higher densities and these correspond to regions where our slit crosses the ring.

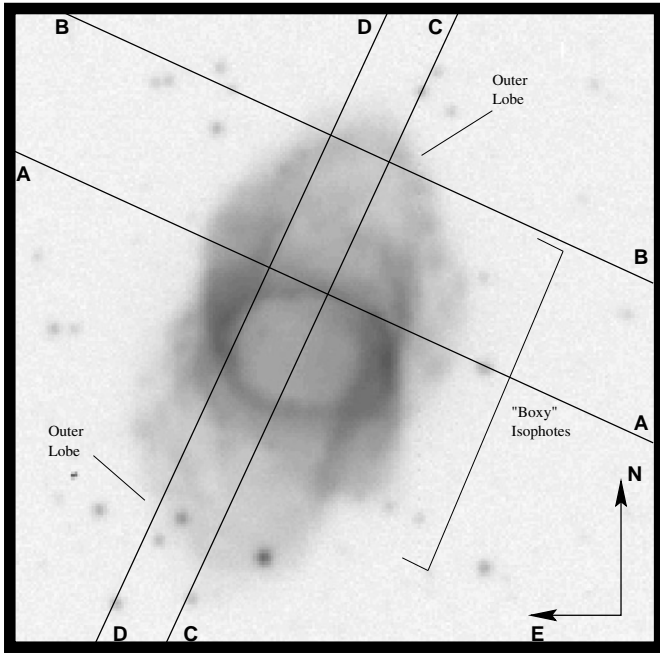


Fig. 2. Greyscale representation of Mz 1 showing the main nebula, central ring and the four longslit positions. The region of “boxy” isophotes, discussed in section 4 on the nebular kinematics, is indicated.

The results of Gaussian fitted line profiles are presented in Fig. 5 for slit position C. This slit position lies most nearly along the major axis of the nebula.

3. Discussion: the central ring

The most conspicuous feature of Mz 1 is the central “ring”. There are two possible structures that could produce this appearance; a central ellipsoidal hollow shell, or a physical ring of material. Examining the longslit position/velocity plots (see Fig. 3) for the slits which cross the ring (C & D) a pronounced increase in intensity of emission can be seen wherever the slit crosses the ring. Only in the slit A observation do we see any evidence of velocity splitting associated with the ring. One side of this is very faint, and we would suggest that the emissions from the strong side come from the ring, whilst the fainter emissions originate from the main nebular structure. The kinematic features in Fig. 3 are consistent with the ring being a radially expanding torus.

The [SII] ratios obtained across the nebula (position C) can be used to determine N_e , the electron density of the gas Osterbrock 1989. The results indicate that the local electron density $N_e = 1700 \pm 600 \text{ cm}^{-3}$ for the ring compared with $N_e = 400 \pm 100 \text{ cm}^{-3}$ in the rest of the nebula (assuming $T_e = 10^4 \text{ K}$). That is, the density of material in the ring area is more than four times that in the core. This density enhancement is also illustrated in Fig. 4, which clearly shows an area of high density emission at the ring position.

Table 2. Measured radial velocities relative to systemic and calculated V_{exp} . The position letters refer to those shown in Fig. 2

Pos'n	Slit	angular offset, θ	$ V_r $ km s $^{-1}$	V_{exp} km s $^{-1}$
1	C	5°	17	23
2	C	5°	17	23
3	D	50°	13	23
4	D	55°	13	24

Therefore it is inferred that the ring is not the edge of a limb brightened shell but an expanding ring of high density gas and we shall interpret our observations in this light.

3.1. Kinematics of the ring

If we assume that the ring is uniformly expanding; then its elliptical appearance is simply a projection effect *i.e.* the ring is tilted. The measured aspect ratio (3:2) indicates an angle of 42° between the plane of the ring and the line of sight.

It can be shown that the relationship between the expansion velocity of an expanding ring and the line-of-sight (radial) velocity is given by :

$$V_{exp} = V_r \left(\frac{\tan^2 \phi + \cos^2 \theta}{\cos^2 \theta} \right)^{\frac{1}{2}}, \quad (1)$$

where V_{exp} is the expansion velocity of the ring, V_r is the observed radial or line-of-sight velocity of the ring, ϕ is the inclination of the plane of the ring to the line-of-sight, θ is the angle made by the observed ellipse minor axis to the line from the geometric centre of this ellipse and the point on its circumference where the velocity observation is made.

From the position/velocity arrays in Figs. 3 and 4 we can estimate the velocity of the gas at the positions where the slit crosses the ring. Given the measured angular offset from the ellipse minor axis Eqn. 1 can be used to calculate the expansion velocity of the ring. Table 2 displays the measured velocities (both as V_{hel} and as velocities relative to the systemic radial velocity) along with measured angular offsets and calculated expansion velocities (V_{exp}).

The results are remarkably consistent and indicate a ring expansion velocity of $23 \pm 2 \text{ km s}^{-1}$. The radius of the ring can be obtained from measurements of the image. In the plane of the ring its radius would be approximately $16''$ ($\equiv 0.16 \text{ pc}$, using a distance to the nebula of 2.0 kpc). We may therefore calculate that the ring is around 6500 years old - assuming a constant expansion rate.

An estimate of the mass of the nebula, knowing the electron density of the ionized gas and the physical size of the ring and the emitting region, may also be made. The nebula is approximately 0.36 pc in diameter by 1.07 pc long. If we consider the emitting volume to be 0.09 pc^3 with an average particle density of 400 cm^{-3} and having a nominal filling factor of 0.1 then we arrive at an ionized mass for the nebula of $0.07 M_{\odot}$, within a

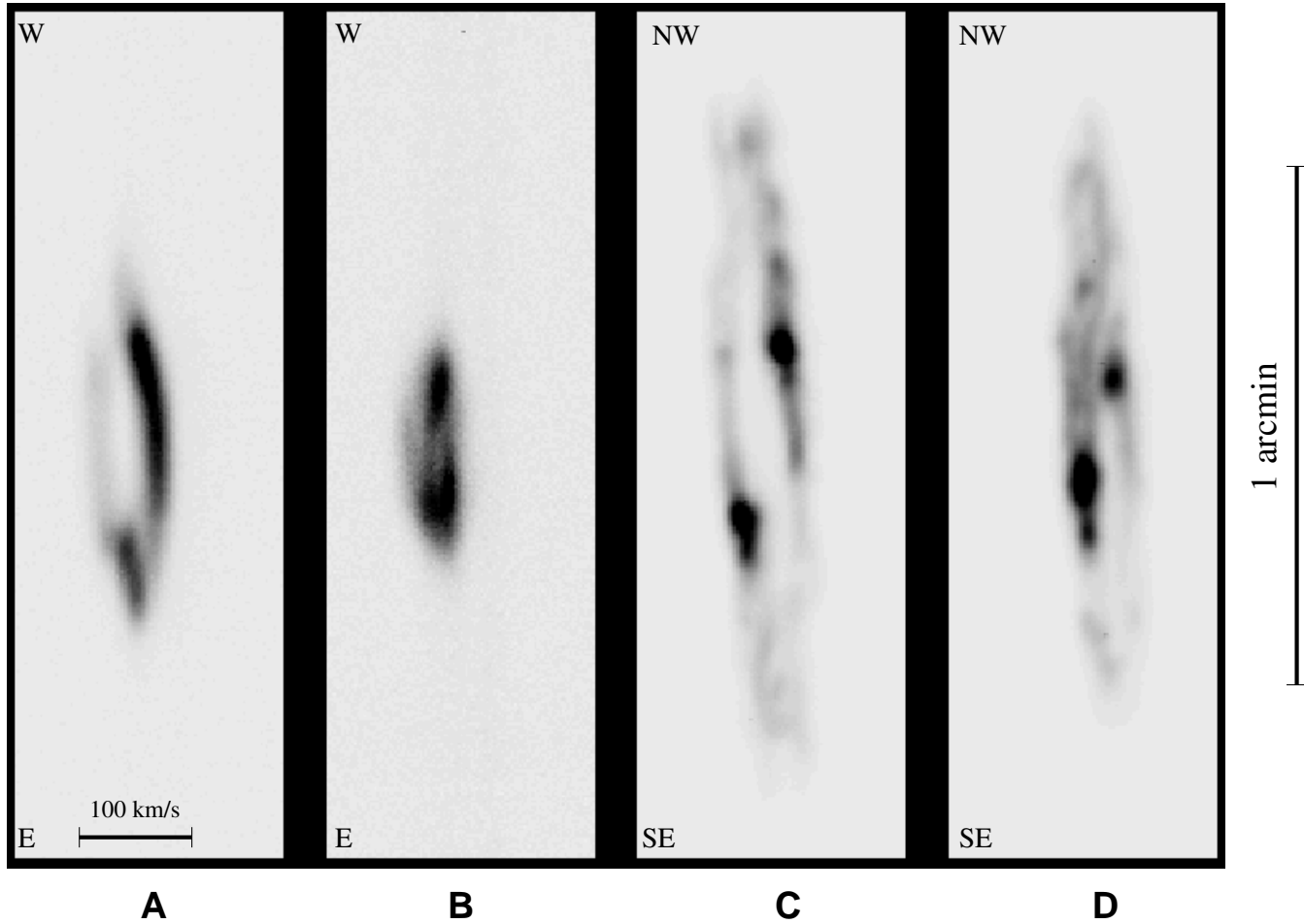


Fig. 3. [NII] 6584 Å position/velocity arrays for the slit positions shown in Fig. 2. Negative radial velocities are to the right.

factor of two. In a similar fashion, assuming an emitting volume is a torus with a radius of 0.16 pc and a thickness of a third of the radius, then a particle density of 1700 cm^{-3} provides an estimated ring mass of $0.01 M_{\odot}$. Again this is within a factor of two under the assumptions made. Mz 1 is also an IRAS point source with 12, 25, and $60 \mu\text{m}$ fluxes of 0.48 Jy, 1.40 Jy and 14.45 Jy respectively (the $100 \mu\text{m}$ flux is an upper limit only for the source). The 25 and $60 \mu\text{m}$ fluxes suggest a dust temperature of 87K. The mass of the nebula would therefore be $0.6 M_{\odot}$, using the model of Marston & Dickens (1988), and assuming a gas-to-dust ratio of 250, a ratio suitable for carbon-rich PN (Siebenmorgen et al 1994). Although it is not known whether Mz 1 is carbon rich or not, the gas-to-dust ratio is certainly expected to be larger than the value of 100 that is typical of the interstellar medium. However, caution should be used here. Some of the emission in the broad IRAS bands will be from emission lines rather than heated dust continuum. Pottasch et al (1984) estimate that as much as 25% of the $25 \mu\text{m}$ emission from planetary nebulae may be associated with emission lines. Assuming a similar value for emission lines in the $60 \mu\text{m}$ band, our IRAS estimate of gas mass is of order $0.5 M_{\odot}$. Further, the continuum $25 \mu\text{m}$ emission is in part due to transiently heated

small grains and at these mid-infrared wavelengths some cool dust and associated gas may remain essentially undetected. The IRAS mass estimate of $0.5 M_{\odot}$ is therefore likely to be a lower limit.

4. Discussion: morphology of the nebula

The loose bipolar structure of the main body of Mz 1 has a major axis oriented along PA 155° . There is only a slight narrowing of the ellipse along its minor axis producing a very mildly ‘waisted’ appearance. The outer edges of the PN near this waist show some enhanced emission intensity. The ring structure appears to be coincident with the ‘waist’ of the nebula but has a width slightly less than it. Slightly fainter lobes of material appear at either end.

The longslit position/velocity graph (Fig. 5) appears as an inclined rectangle for the inner bipolar with “boxy” isophotes, with the lobes showing velocity splitting beyond this.

Corradi & Schwarz (1993) have shown that a good fit to the sort of ‘inclined rectangular’ velocity field seen here can be obtained by using an expanding cylinder model. In this model, the expansion velocity at any point on the surface of a cylinder

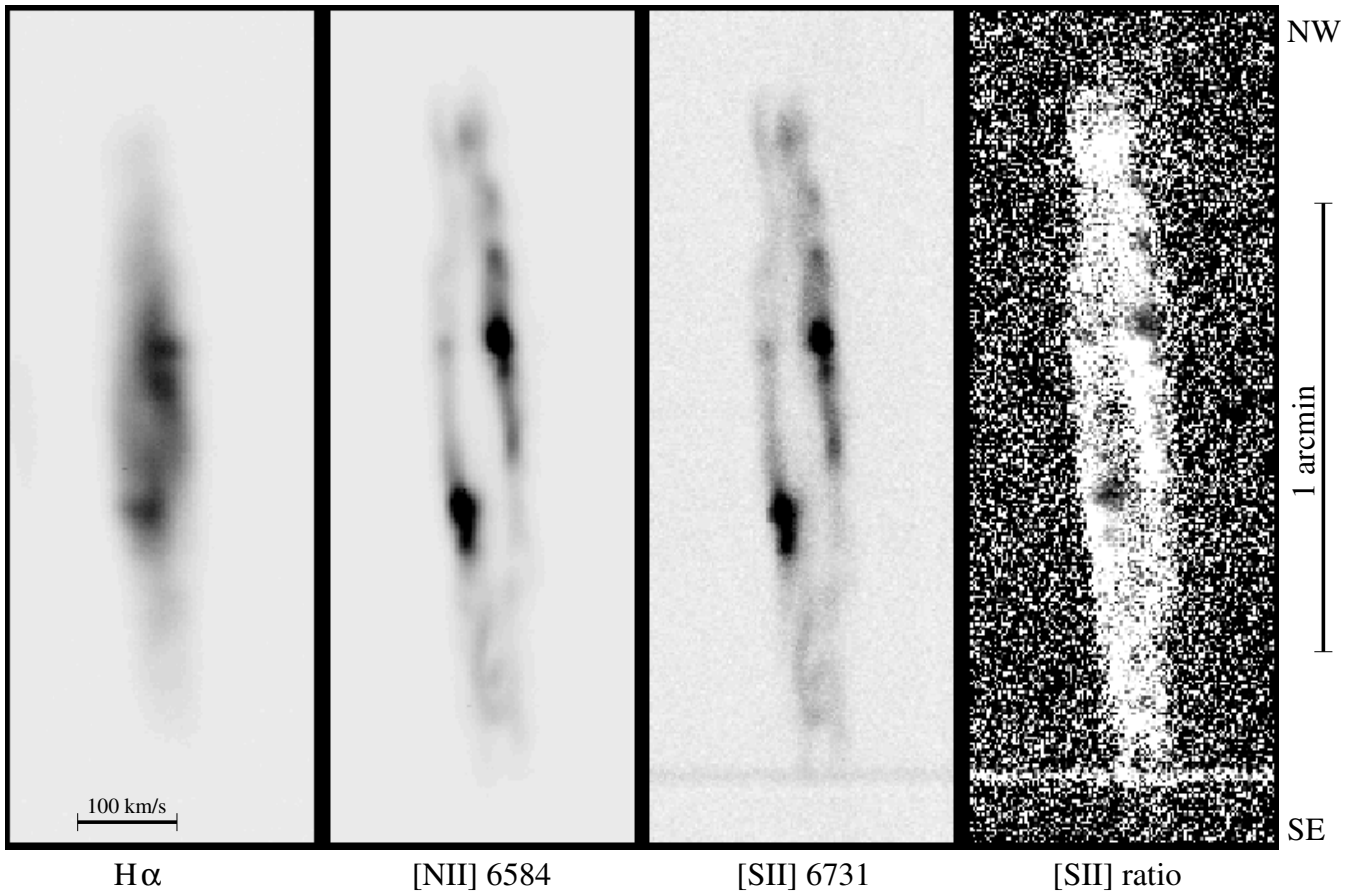


Fig. 4. Position-velocity arrays of the $H\alpha$, $[NII] 6584 \text{ \AA}$ and $[SII]$ emissions from slit position C. The right hand panel corresponds to the $[SII] 6717 \text{ \AA} / [SII] 6731 \text{ \AA}$ ratio and provides an indication of the electron density present in the emitting gas. The dense ring appears as a darker patch. Negative radial velocities are to the right.

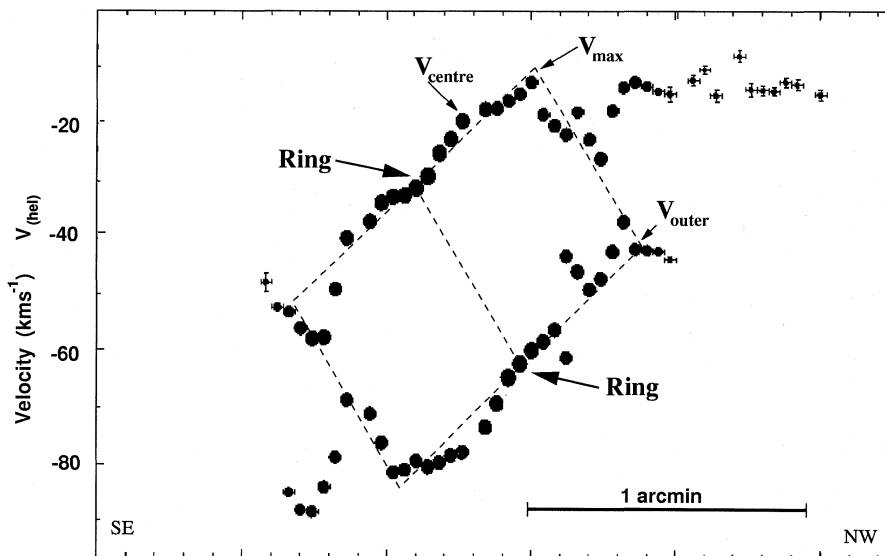


Fig. 5. Position/velocity curve for the $[NII] 6584 \text{ \AA}$ line profiles along slit position C. Superimposed is a fit for the cylindrical model used in Sect. 4, together with the key velocities referred to in equations 2 to 4.

is considered to be time-independent, directed radially outward and proportional to the length of the vector joining the centre with that point (see Fig. 6).

The following equations describe the velocity field :

$$V_{max} = V_y \cos(i) + V_x \sin(i) \quad (2)$$

$$V_{outer} = V_y \cos(i) - V_x \sin(i) \quad (3)$$

$$V_{centre} = \frac{V_x}{\sin(i)} \quad (4)$$

where i is the inclination of the axis of the cylinder with respect to the line-of-sight, V_y is the expansion velocity along the axis of the cylinder, V_x is the expansion velocity along the radius of the cylinder, V_{max} is the maximum radial velocity observed, V_{outer} is the radial velocity measured at the furthest observed distance from the centre, V_{centre} is the radial velocity observed towards the center of the nebula (see Fig. 6).

A best fit parallelogram was overlaid onto the position-velocity diagram of Fig. 5 and the appropriate values measured from this. The equations above were then used to calculate i , V_x and V_y , giving $i = 47 \pm 3^\circ$, $V_x = 22 \pm 3 \text{ km s}^{-1}$ and $V_y = 32 \pm 3 \text{ km s}^{-1}$. The expansion of the nebula in the x direction for this cylindrical model is therefore consistent with the ring expansion velocity, $V_{exp} = 23 \pm 2 \text{ km s}^{-1}$ (see sect. 3.1).

These values can be used to calculate a spatial aspect ratio of 1.5:1 for the inner, bipolar portion of the lobes. This does in fact match the ‘‘boxy’’ isophotes of the image quite well. The outer, extended components show expansion away from each other of $\approx 66 \text{ km s}^{-1}$ (in the plane of the nebula). In order to become 1.07 pc apart would therefore require 16,000 years, for a constant expansion rate.

The timescale for the formation of all of the central features of Mz 1 are similar (6 - 7,000 years). The outer lobes may have taken somewhat longer to form and possibly preceded the formation of the expanding ring and barrel-like (‘‘boxy’’) feature of the main body of the nebula. However, we have assumed a constant expansion velocity. Bujarrabal et al (1994) suggest that expansion velocities for planetary nebulae may increase with age, especially after the ionization front passes through. Mz 1 may therefore be even older than the age quoted here.

5. Discussion: formation of the bipolar

It would be natural to assume that the ring is part of the formation mechanism of the nebula - or at least is the remnants of an equatorial density enhancement that helped form the nebula. In the latter case we could speculate that a ‘‘disk’’ of enhanced density gas around the equator of the progenitor star produced the bipolarity of the nebula and an expanding shell sweeping up this disk could produce an expanding ring.

We now consider the formation of the bipolar flow in the context of the evolution of the central star. Prior to its existence as a hot central star with a fast wind (several hundred km s^{-1}) and relatively low mass-loss rate ($\sim 10^{-8} M_\odot \text{ yr}^{-1}$), the central

star is expected to have passed through

(a) An AGB phase with mass loss rates around $10^{-6} M_\odot \text{ yr}^{-1}$ and wind speeds of typically 10 - 15 km s^{-1} . (b) A superwind phase with mass-loss rates jumping by a factor of 10 - 20 for a period of typically 10,000 years (see e.g. Mellema 1995).

These two phases can apparently alternate and a clean separation between the two phases does not hold (Izumiura, 1997; Zijlstra et al 1992).

5.1. Formation of the bipolar via a fast wind

We may speculate on the origins of the observed velocity features in the context of interacting stellar winds in which a superwind follows the AGB phase and is in turn interacted with by the fast wind of the central star when a planetary nebula is formed. Several papers have recently been produced on the hydrodynamics of fast winds from an evolving star interacting with prior AGB and superwind phase materials. If a density contrast exists in the circumstellar material between the equator and poles of the star, primarily from the material emitted in the prior superwind phase, then bipolar outflows become probable in the ensuing fast wind phase (Mellema 1993; 1995). Mz 1 is much larger and slower in expansion than in the hydrodynamical models of Mellema (1993) or Frank (1994). Even allowing for a distance overestimate of a factor of 2, Mz 1 is significantly larger than the grids they consider. This produces some problems in that the contrast between high and low density regions around the star produced in the superwind phase is expected to become smoothed out over time. Mellema & Frank (1995) indicate that there is only a limited time for aspherical bubble formation and as a consequence slowly evolving nebulae are expected to be rounder. However, the size of Mz 1 (0.54 pc) means that this smoothing timescale should be 48,000 years, far longer than the time taken to form the nebula.

Mellema (1995) has modelled the morphology and kinematics of PNe expanding into environments with axisymmetric density gradients formed in earlier superwind phases. We may consider a scaled-up version of case D from Mellema (1995), with Mz 1 almost a factor of 10 larger than that simulated. The velocity-position map obtained for Mz 1 is morphologically similar to that of the simulation for a 30° tilt to the line-of-sight (see Fig. 13 in Mellema 1995). Not all properties of this simulation are observed, though there is no obvious evidence in our observations for triple velocity components (expected at $\pm 0.16 \text{ pc}$ from the centre of Mz 1 in a scaled-up simulation).

Considering the length of the nebula to be 1.07 pc, then a superwind of 10 - 25 km s^{-1} should take between 20,000 and 48,000 years to expand out to this distance. Allowing 7,000 years for the nebula formation, the superwind phase should be of order 13,000 to 41,000 years, with a faster superwind lasting a shorter time. With an old bipolar, it becomes more likely that the nebula has penetrated beyond the edge of the superwind distribution into much lower density AGB wind material. This may well be occurring in the lobes at the end of the Mz 1 bipolar, where there is a suggestion of a faster flow. In this case, the edge of the superwind surroundings, which shape the bipolar,

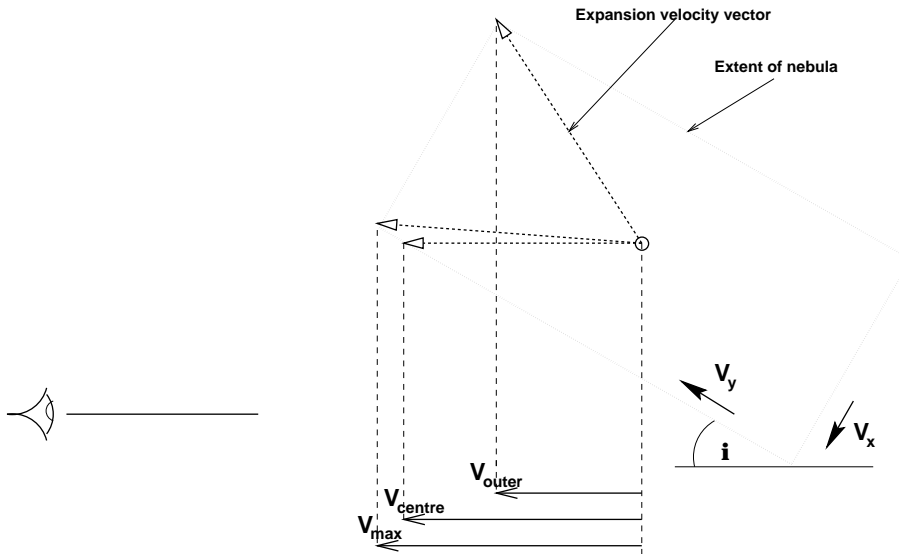


Fig. 6. Diagram showing the cylindrical model velocity field with key observational velocities marked

may only stretch to the edge of the “boxy” isophotes (fitted by the velocity-position rectangle in Fig. 5). In order to get to this radius, the expansion time for the superwind would need to be between 2,000 and 16,000 years. Indeed, for a 15 km s^{-1} superwind, the timescale for the flow is estimated to be 8,000 years.

However, the mass-loss rate for this wind would need to be high. If we take the mass of the nebula to be $0.5 M_{\odot}$ then the mass-loss rate in the superwind would be $6 \times 10^{-5} M_{\odot} \text{ yr}^{-1}$ for a 8,000 year superwind. Further mass, lost in the superwind phase, is expected to still reside exterior to the bipolar (particularly in the equatorial regions), yet to be swept up. Our calculated mass loss rate is therefore a lower limit.

5.2. Formation of the bipolar structure by the superwind

The period of formation for the nebula, 7,000 years, the speed of the nebula 22 km s^{-1} at the equator and 32 km s^{-1} at the poles, plus the estimated mass-loss rate to form the nebula over a 7,000 year timescale ($\geq 7 \times 10^{-5} M_{\odot} \text{ yr}^{-1}$) are similar parameters to those expected in the superwind phase of evolution. If an equatorial disc of material were to have existed prior to the superwind mass ejection, then a bipolar outflow would ensue. Material in the outer parts of the lobes of Mz 1 appear more collimated, and there is some suggestion from our kinematics that the outer parts to the lobes of the nebula are older than the main, cylindrically expanding, component of the nebula. We might therefore suggest an evolution along the following lines.

- (i) A collimated AGB outflow at a relatively low mass-loss rate, restricted by a pre-existing disk.
- (ii) As a relatively fast superwind stage begins, the wind luminosity increases allowing the collimating disc to be swept up in a general expansion.
- (iii) A decreasing amount of collimation of the wind leads to the wider (“boxy”) isophotes.
- (iv) The material is ionized by the central star.

(v) The fast wind of the planetary central star may then begin to sweep up material *inside* the bipolar structure. The filling seen at low velocities in $H\alpha$ can be interpreted as indicating that the fast wind has evacuated little of the bipolar so far.

Advantages of this model include the (at least partial) filling of the interior of the nebula with a slow, dense stellar wind. Such a situation is suggested by the $H\alpha$ position-velocity map in Fig. 4, which indicates that the interior of the nebula is filled. This is not well explained in the fast wind formation mechanism modelled by Mellema (1995) and Frank (1994), where a low density cavity is expected to be produced. The timescale for the formation of Mz 1 is similar to that expected for the superwind phase occurring immediately prior to the fast wind phase. Finally, the expansion velocity and estimated mass-loss rates are also not out of line with those expected from the superwind phase (Habing 1990; Blöcker & Schönberner, 1991).

5.3. Comparison with Fleming 1

It is interesting to compare Mz 1 to the structure of the core of Fleming 1 (López, Meaburn & Palmer, 1995; Palmer et al. 1996). In both cases the main body of the PN appears to be a well developed, bipolar structure (coincidentally inclined to the line-of-sight by approximately the same amount) with an expanding ring about its waist. In the case of Mz 1 the spectacular jet-like features observed in Fleming 1 do not appear to be present or have not been covered by our slit positions. Fleming 1 also displays older “outer lobes” formed at the end of the barrel-shaped structure of the nebula. The kinematics of the Fleming 1 nebula suggests that the ring expansion started around 9,000 years ago, a slightly longer time scale than for the formation of Mz 1, although the general expansion of the torus is 36 km s^{-1} , a somewhat faster rate than for Mz 1 and faster than might be expected from a superwind phase.

6. Conclusions

One of the major features of this nebula is the relatively slow expansion it has, suggesting quite a large overall age. Observations of such a nebula can allow the detection of dynamical components associated with changes occurring in the wind from the central star.

The morphology of the main nebula has been shown to be well modelled as a cylinder with its axis inclined at an angle of $47^\circ \pm 3^\circ$ to the line of sight. The ring structure, which appears at the centre of the nebula, has been shown to be expanding in a plane with an angle of inclination to the line of sight of 42° . This means that the ring's axis of radial symmetry is inclined at an angle of 48° to the line of sight, almost identical to that of the main nebula. We conclude that the kinematics of the nebula Mz 1 show the main part of the nebula to have cylindrical expansion of $22 \pm 3 \text{ km s}^{-1}$ at the equator and $32 \pm 3 \text{ km s}^{-1}$ at the poles. The ring of denser material about the waist of the bipolar has a similar expansion rate to that of the main nebula (within our errors). A dynamical age for the formation of the ring and main bipolar of $7,000 \pm 1,000$ years (for the assumed distance of 2.0kpc) is implied. The extended outer portions of the lobes which stretch beyond the cylindrically expanding component may well have been ejected at an earlier date. Incidentally, the Helix nebula (NGC 7293) appears to have a similar morphological and kinematical structure, but with the ring expanding closer to the plane of the sky to provide the helical feature Meaburn et al. 1997.

Similarities exist between the observed morphological and kinematical properties of Mz 1 and the models of Mellema (1993; 1995) and Frank (1994). The outer lobes appear to stretch beyond the main body of a superwind environment, which may be marked by the "boxy" isophotes. A 15 km s^{-1} superwind could set up such an environment in 8,000 years although a mass-loss rate of more than $6 \times 10^{-5} M_\odot \text{ yr}^{-1}$ is required. A disadvantage to this model is that it does not explain why Mz 1 appears to be filled with $\text{H}\alpha$ emitting material. It is expected that the fast wind formation mechanism (used in the models of Mellema and Frank) has *not* swept out a cavity.

A filled bipolar may be produced by assuming that the material interior to Mz 1 has come from a slow rather than fast wind. In this case we may postulate that it comes from the superwind phase itself, rather than having been swept up by the following fast wind phase, in which case an equatorial disk structure would have to have been produced prior to the superwind phase. Material ejected prior to and at the beginning of the superwind phase would then be collimated, producing the outer lobes. As the wind luminosity increases at the start of the superwind, the disc of material is swept away and the flow becomes less collimated producing the wider hourglass shape. We find that the timescale, expansion velocity and mass-loss rates needed to create the nebula are not inconsistent with stellar parameters expected from a superwind phase of evolution.

Whether a disk of material exists prior to the superwind phase of evolution of the central star of Mz 1 or not, it appears

that a high mass-loss rate is required for the formation of the nebula ($\geq 5 \times 10^{-5} M_\odot \text{ yr}^{-1}$).

Acknowledgements. We would like to thank the staff of the AAT for their excellent help at the telescope. JAL acknowledges continued support from CONACYT and DGAPA-UNAM. APM thanks NASA JOVE for support under grant NAG8-264. Plus support from a NASA grant administered by the American Astronomical Society. Astronomical computing facilities at the University of Manchester were provided by STARLINK.

References

- Blöcker T., Schönberner D., 1991, *A&A*, 244, L43
 Bujarrabal V., Alcolea J., Neri R., Grewing M., 1994, *ApJ*, 436, L169
 Cahn J. H., Kaler J. B., Stanghellini L., 1992, *ApJS*, 94, 399
 Corradi L. M., Schwarz H. E., 1993, *A&A*, 273, 747
 Frank A., 1994, *AJ*, 107, 261
 Habing H., 1990, in *From Miras to Planetary Nebulae*, Mennessier, M. O., Omont A., eds., Editions Frontières, Gif-sur-Yvette, p.16
 Icke V., 1988, *A&A*, 202, 177
 Izumiura H., 1997, *A&A*, 232, 449
 Kwok S., Purton C. R., Fitzgerald P. M., 1978, *ApJ*, 219, L125
 López J. A., Meaburn J., Palmer J. W., 1995, *ApJ*, 415, L135
 Marston A. P., Dickens, R. J., 1988, *A&A*, 193, 27
 Meaburn J., Blundell B., Carling R., Gregory D. F., 1984, *MNRAS*, 210, 463
 Meaburn J., Clayton C. A., Bryce M., Walsh J. R., Holloway A. J., Steffen W., 1997, *MNRAS*, in press.
 Mellema G., 1993, Numerical models for the formation of aspherical planetary nebulae. Ph. D. thesis, University of Leiden
 Mellema G., 1995, *MNRAS*, 277, 173
 Mellema G., Frank A., 1995, *MNRAS*, 273, 401
 Osterbrock D. E., 1989, *Astrophysics of Gaseous Nebulae*, University Science Books.
 Palmer J. W., López J. A., Meaburn J., Lloyd H. M., 1996, *A&A*, 307, 225
 Pottasch S. R., Baud B., Beintema D., Emerson J., Habing H. J., Harris S., Houck J., Jennings R., Marsden P., 1984, *A&A*, 138, 10
 Shortridge K., 1991, FIGARO - General Data Reduction and Analysis. SERC STARLINK, RAL
 Siebenmorgen R., Zijlstra A. A., Krugel E., 1994, *MNRAS*, 271, 449
 Van de Steene G. C., Zijlstra A. A., 1994, *A&AS*, 108, 485
 Wilkins T. N., Axon D. J., 1991, SUN 16.3. SERC STARLINK, RAL
 Zhang C. Y., 1995, *ApJS*, 98, 659
 Zijlstra A. A., Loup C., Waters L. B. F. M., De Jong T., 1992, *A&A*, 265, L5